

## Assessment of CMIP5 climate models and projected temperature changes over Northern Eurasia

This content has been downloaded from IOPscience. Please scroll down to see the full text.

2014 Environ. Res. Lett. 9 055007

(<http://iopscience.iop.org/1748-9326/9/5/055007>)

View [the table of contents for this issue](#), or go to the [journal homepage](#) for more

Download details:

IP Address: 169.234.63.136

This content was downloaded on 28/05/2014 at 19:05

Please note that [terms and conditions apply](#).

# Assessment of CMIP5 climate models and projected temperature changes over Northern Eurasia

Chiyan Miao<sup>1</sup>, Qingyun Duan<sup>1</sup>, Qiaohong Sun<sup>1</sup>, Yong Huang<sup>2</sup>,  
Dongxian Kong<sup>1</sup>, Tiantian Yang<sup>3</sup>, Aizhong Ye<sup>1</sup>, Zhenhua Di<sup>1</sup> and Wei Gong<sup>1</sup>

<sup>1</sup> State Key Laboratory of Earth Surface Processes and Resource Ecology, College of Global Change and Earth System Science, Beijing Normal University, Beijing 100875, People's Republic of China

<sup>2</sup> Appraisal Center for Environment & Engineering, Ministry of Environmental Protection, Beijing 100012, People's Republic of China

<sup>3</sup> Department of Civil and Environmental Engineering, University of California, Irvine, CA 92697, USA

E-mail: [miaocy@vip.sina.com](mailto:miaocy@vip.sina.com)


Received 3 January 2014, revised 14 April 2014

Accepted for publication 23 April 2014

Published 28 May 2014

## Abstract

Assessing the performance of climate models in surface air temperature (SAT) simulation and projection have received increasing attention during the recent decades. This paper assesses the performance of the Coupled Model Intercomparison Project phase 5 (CMIP5) in simulating intra-annual, annual and decadal temperature over Northern Eurasia from 1901 to 2005. We evaluate the skill of different multi-model ensemble techniques and use the best technique to project the future SAT changes under different emission scenarios. The results show that most of the general circulation models (GCMs) overestimate the annual mean SAT in Northern Eurasia and the difference between the observation and the simulations primarily comes from the winter season. Most of the GCMs can approximately capture the decadal SAT trend; however, the accuracy of annual SAT simulation is relatively low. The correlation coefficient  $R$  between each GCM simulation and the annual observation is in the range of 0.20 to 0.56. The Taylor diagram shows that the ensemble results generated by the simple model averaging (SMA), reliability ensemble averaging (REA) and Bayesian model averaging (BMA) methods are superior to any single GCM output; and the decadal SAT change generated by SMA, REA and BMA are almost identical during 1901–2005. Heuristically, the uncertainty of BMA simulation is the smallest among the three multi-model ensemble simulations. The future SAT projection generated by the BMA shows that the SAT in Northern Eurasia will increase in the 21st century by around 1.03 °C/100 yr, 3.11 °C/100 yr and 7.14 °C/100 yr under the RCP 2.6, RCP 4.5 and RCP 8.5 scenarios, respectively; and the warming accelerates with the increasing latitude. In addition, the spring season contributes most to the decadal warming occurring under the RCP 2.6 and RCP 4.5 scenarios, while the winter season contributes most to the decadal warming occurring under the RCP 8.5 scenario. Generally, the uncertainty of the SAT projections increases with time in the 21st century.

 Online supplementary data available from [stacks.iop.org/ERL/9/055007/mmedia](http://stacks.iop.org/ERL/9/055007/mmedia)

Keywords: CMIP5, multi-model ensembles, Northern Eurasia, temperature



Content from this work may be used under the terms of the [Creative Commons Attribution 3.0 licence](http://creativecommons.org/licenses/by/3.0/). Any further distribution of this work must maintain attribution to the author(s) and the title of the work, journal citation and DOI.

Global atmospheric concentrations of greenhouse gases have significantly increased since the pre-industrial era. The increasing concentration of greenhouse gases is an important reason for global warming from the last century with high confidence (Yang *et al* 2011). During the 20th century, the average surface air temperature (SAT) of the Northern Hemisphere has risen approximately 1 °C (IPCC 2007, Polyakov *et al* 2012). As outlined in the fourth assessment report (AR4) of the Intergovernmental Panel on Climate Change (IPCC), even if greenhouse gases are stabilized at the level in 2000, the average global temperature will increase approximately 0.1 °C every decade (IPCC 2007).

Increases in the temperature may have serious influence on the natural and social aspects, such as water availability (Piao *et al* 2007, Gosling and Arnell 2011, Miao *et al* 2009, Sheffield *et al* 2012), food security (Tubiello *et al* 2007, Lobell *et al* 2008, Piao *et al* 2010), ecological environment (Allen *et al* 2010, Miao *et al* 2010, Tabari *et al* 2013, Yang *et al* 2013, Yang *et al* 2014), species biodiversity (Wake and Vredenburg 2008, Nowak 2010), and human health (Robine *et al* 2008, Gosling *et al* 2009) etc. These influences have urged the scientific and social communities to improve understanding of the causes and consequences of global warming (Sun *et al* 2014). Moreover, policymakers need the latest information on the likely future impacts of climate change to reconcile human society with natural systems.

Northern Eurasia accounts for about 20% of the Earth's land surface and 60% of the terrestrial land cover north of 40°N (Groisman *et al* 2009). It contains vast areas of wetlands, especially peatland, which contains a large amount of organic carbon and is often underlain by continuous and discontinuous permafrost (Zhu *et al* 2011). Compared with low latitude regions, Northern Eurasia, especially its northern areas, has been under more dramatic environmental changes in the 20th century, including increasing temperatures, melting permafrost, changing precipitation and prolonged growing seasons (Romanovsky *et al* 2007, IPCC 2007). According to observation, Northern Eurasia is the region with the largest and the steadiest SAT increases, and warming became most pronounced during the second half of the 20th century (Groisman *et al* 2007). During the period of widespread instrumental observations in Northern Eurasia (since 1881), the annual surface air temperature has increased 1.5 °C (while 3 °C in the winter season) (Groisman and Soja 2009). There is a statistically significant increase in the number of thaw days over Northern Eurasia (McBean *et al* 2005), which is primarily due to the reduction of days with frost, ice and remnant snow on the ground rather than due to the snow cover retreat (Groisman *et al* 2006). However, there is an interesting phenomenon in Northern Eurasia found by Bulygina *et al* (2011) that most areas of Northern Eurasia have experienced an increase in both winter average and maximum snow depths in recent decades, which is against the background of global temperature rise and sea ice reduction in the northern hemisphere.

Climate projections and their associated applications have become an important topic during recent decades. Several research teams around the world develop models to

simulate the current climate and its future evolution under different greenhouse gas and aerosol scenarios (Buser *et al* 2009). Global coupled Atmospheric-Ocean General Circulation Models (coupled GCMs) are the modeling tools traditionally used in theoretical investigations of climatic change mechanisms (Covey *et al* 2003). By using GCMs, we can not only simulate the present-day and project future climatic changes under different scenarios but also separate natural climate variability from anthropogenic effects.

The GCMs simulations for the fifth assessment report (AR5) of the IPCC have recently become available (Taylor *et al* 2012). Comparing to the IPCC AR4, the GCMs in AR5 include a more diverse set of model types (i.e., climate/Earth system models with more interactive components such as atmospheric chemistry, aerosols, dynamic vegetation, ice sheets and carbon cycle) (Liu *et al* 2013). A number of improvements in the physics, numerical algorithms and configurations are implemented in the IPCC AR5 models with a new set of scenarios called representative concentration pathways (RCPs) used in the AR5 simulations (Moss *et al* 2010). The RCPs span a large range of stabilization, mitigation and non-mitigation pathways. Consequently, the range of the temperature estimates is larger than that of the scenarios in the AR4, which only covers non-mitigation scenarios (Rogelj *et al* 2012). It is expected that some of the scientific questions that occur during the preparation of the IPCC AR4 will be addressed in the AR5 (Taylor *et al* 2012).

The climate change in Northern Eurasia is a topic of great interest, and the amount of research associated with the GCMs is developed. However, previous analyses are primarily focused on the early experiments of the IPCC. An evaluation and application of the updated generation of the AR5 GCMs in Northern Eurasia is missing. In this study, we focus on the state-of-the-art models that have been made publically available through the Coupled Model Inter-comparison Project phase 5 (CMIP5). This study is aimed at answering the following questions: 1) how well do the AR5 GCMs reproduce the historical SAT patterns; 2) which type of multi-model ensemble techniques can provide the best skill to improve the simulation performance; and 3) what changes in climate means may be expected in the future. Our results potentially provide inputs for climate change impact assessments that explore the probability of climate-related threats in Northern Eurasia.

## 1. Data and methods

### 1.1. Data

Observations of monthly SAT over Northern Eurasia are obtained from the Climate Research Unit data (CRU TS 3.1) (Mitchell and Jones 2005, Harris *et al* 2013) (available at <http://badc.nerc.ac.uk/data/cru/>). The horizontal resolution of the dataset is 0.5° × 0.5°, and the time period in this research is from 1901 to 2005.

24 GCMs outputs obtained from the CMIP5 data archive (<http://cmip-pcmdi.llnl.gov/cmip5/index.html>) are listed in

**Table 1.** List of the global climate models in IPCC-AR5.

GCM	Model	Resolution	Source
1	BCC- CSM 1.1	64 × 128	Beijing Climate Center, China Meteorological
2	BCC- CSM1.1 (m)	160 × 320	Administration, China
3	BNU-ESM	64 × 128	Beijing Normal University, China
4	CanESM2	64 × 128	Canadian Centre for Climate Modelling and Analysis, Canada
5	CCSM4	192 × 288	National Center for Atmospheric Research (NCAR), USA
6	CNRM- CM5	128 × 256	Centre National de Recherches Meteor- ologiques, France
7	CSIRO- Mk3.6.0	96 × 192	Australian Common- wealth Scientific and Industrial Research Organisation
8	FGOALS- g2	108 × 128	Institute of Atmospheric Physics, Chinese Academy of Sciences, China
9	FIO-ESM	64 × 128	The First Institute of Oceanography, SOA, China
10	GFDL- CM3	90 × 144	Geophysical Fluid Dynamics Laboratory , USA
11	GFDL- ESM2G	90 × 144	
12	GISS-E2-H	90 × 144	Goddard Institute for Space Studies (NASA), USA
13	GISS-E2-R	90 × 144	
14	HadGEM2- ES	145 × 192	Met Office Hadley Centre, UK
15	IPSL- CM5A- LR	96 × 96	Institut Pierre-Simon Laplace, France
16	IPSL- CM5A- MR	143 × 144	
17	MIROC5	128 × 256	Atmosphere and Ocean Research Institute, University of Tokyo, Japan
18	MIROC- ESM	64 × 128	Japan Agency for Mar- ine-Earth Science and Technology, Atmo- sphere and Ocean Research Institute (The University of Tokyo), Japan
19	MIROC- ESM- CHEM	64 × 128	
20	MPI- ESM-LR	96 × 192	Max Planck Institute for Meteorology (MPI- M), Germany
21	MPI- ESM-MR	96 × 192	
22	MRI- CGCM3	160 × 320	Meteorological Research Institute, Japan

**Table 1.** (Continued.)

GCM	Model	Resolution	Source
23	NorESM1- M	96 × 144	Norwegian Climate Centre, Norway
24	NorESM- ME	96 × 144	

table 1. The monthly data includes the historical (1901–2005) and the future (2006–2099) periods. Here we focus on the SAT projection under three scenarios (i.e., RCP 2.6, RCP 4.5 and RCP 8.5). The three RCPs represent ‘low’ (RCP 2.6), ‘medium’ (RCP 4.5) and ‘high’ (RCP 8.5) scenarios featured by the radiative forcings of 2.6, 4.5 and 8.5 W m<sup>-2</sup> by 2100, respectively. The CO<sub>2</sub>-equivalent concentrations in the year 2100 for RCP 2.6, RCP 4.5 and RCP 8.5 are 421 ppm, 538 ppm and 936 ppm, respectively (Meinshausen *et al* 2011). For comparison purpose, all GCM outputs are regridded to the same resolution as that of the observed data (0.5° × 0.5° grid).

### 1.2. The methodology of multi-model ensemble averaging

Because single models are overconfident (Weigel *et al* 2008) and multi-model ensembles contain information from all participating models (Pincus *et al* 2008), it is generally believed that multi-model ensembles are superior to single models (IPCC 2001, Duan and Phillips 2010, Miao *et al* 2013). In this study, three types of popular ensemble methods are used. They are simple model averaging (SMA), reliability ensemble averaging (REA) and Bayesian model averaging (BMA) techniques.

SMA is the simplest multi-model ensemble technique. Each model has the same weight ( $w_k = 1/K$ , where  $K$  is the number of models) in the multi-model forecast. When using the SMA, any knowledge about the performance of the model is neglected (Casanova and Ahrens 2009).

The REA is a weighted average of ensemble members method based on the ‘reliability’ of each model (Giorgi and Mearns 2002). The reliability factor of the  $k$ th model ( $R_k$ ) takes into account of the ability of each ensemble member to simulate the observed climate ( $R_B$ ) and its degree of convergence in the projected climate change with respect to the other models in the ensemble ( $R_D$ ).

$$R_k = \left[ (R_{B,k})^m \times (R_{D,k})^n \right]^{1/(m \times n)}$$

$$= \left[ \left( \frac{\varepsilon}{|B_k|} \right)^m \times \left( \frac{\varepsilon}{D_k} \right)^n \right]^{1/(m \times n)} \quad (1)$$

$$w_k = \frac{R_k}{\sum R} \quad (2)$$

where  $R_B$  is a factor that is inverse proportional to the absolute bias ( $B$ ) in simulating the present-day variable and  $R_D$  is a factor that measures the model reliability in terms of the

distance ( $D$ ) of the change calculated by a given model from the REA average change. The parameters  $m$  and  $n$  are the weights of the model performance criterion ( $R_B$ ) and the model convergence criterion ( $R_D$ ), respectively, which are typically equal to 1. The parameter  $\varepsilon$  in equation (1) is the natural variability of the climatic variable. More details of the REA process are provided in Giorgi and Mearns (2002) and Mote and Salathé (2010).

The BMA generates a probability density function (PDF), which is a weighted average of the PDFs centered on the forecasts. The BMA weights reflect the relative contributions of the component models to the predictive skill over a training sample. The combined forecast PDF of a variable  $y$  is:

$$p(y|y^T) = \sum_{k=1}^K p(y|M_k, y^T) p(M_k|y^T) \quad (3)$$

where  $p(y|M_k, y^T)$  is the forecast pdf based on the model  $M_k$  alone, estimated from the training period of observations  $y^T$ ; and  $K$  is the number of models combined.  $p(M_k|y^T)$  is the posterior probability of the model  $M_k$  corrected using the training data. This term is computed based on Bayes' theory:

$$p(M_k|y^T) = \frac{p(y^T|M_k)p(M_k)}{\sum_{l=1}^K p(y^T|M_l)p(M_l)} \quad (4)$$

The BMA weights are estimated using the maximum likelihood (Raftery et al 2005). To estimate given parameters, the likelihood function is the probability of the training data and is viewed as a function of the parameters (Yang et al 2011). The weights are chosen to maximize this function (i.e., the parameter values for which the observation data are most likely to have been observed). The algorithm used to calculate the BMA weights and variance is called the expectation maximization (EM) algorithm (Dempster et al 1977). More details of the BMA process are provided in Raftery (2005) and Duan and Phillips (2010).

### 1.3. Evaluation process

For GCM performance assessment, the bias between observation and model simulations is compared. The SAT change during the historical period (1901–2005) and the projected future scenarios (2006–2099) are analyzed.

In order to evaluate the ensemble performance, the Taylor diagram technique is used. The Taylor diagram is quantified in terms of the correlation ( $R$ ), the centered root-mean-square-error ( $RMSE$ ) and the amplitude of the standard deviations ( $Std$ ). The diagram provides a way of graphically summarizing how closely a pattern matches observations (Taylor 2001). Moreover, the uncertainty of the different multi-model ensembles is also compared. Here, we calculate

the standard deviation of the changes,  $\delta$ , defined by

$$\delta = \left[ \frac{\sum_{k=1}^K w_k (T_k - En)^2}{\sum_{k=1}^K w_k} \right]^{1/2} \quad (5)$$

where ( $w_k$ ) is the weight of  $k$ th model generated by different multi-model ensemble techniques,  $T_k$  is the  $k$ th model output and  $En$  is the ensemble. The upper and lower uncertainty limits are thus defined as:

$$Upper = En + \delta \quad (6)$$

$$Lower = En - \delta \quad (7)$$

If the changes are distributed as a Gaussian PDF, the  $\pm\delta$  range implies a 68.3% confidence interval.

### 1.4. Temperature projection

It is generally accepted that the agreement between models and observations currently is the only way to assign confidence into the quality of a model (Errasti 2011), and the better a model performance in reproducing present-day climate, the higher the reliability of the climate change simulation (Giorgi and Mearns 2002, Coquard et al 2004). Each GCM's weight can be obtained from the ensemble process during the period of 1901–2005. Applying with these weights, multi-model ensemble projections in temperature over the 21st century scenarios can be generated.

## 2. Results

### 2.1. Model bias and warming trend

Figure 1 shows the bias in 24 CMIP5 climate models by comparing the observed and simulated data of the 105 year annual and seasonal mean temperatures. Most of the GCMs give reasonably accurate predictions of the mean temperature. Among the 24 GCMs, nine models underestimate the annual mean temperature, while the others overestimate. The maximum bias for SAT simulation comes from the FGOALS-g2 model, with a value of  $-4.31$  °C. The BCC-CSM 1.1 and GISS-E2-R models perform the best, with a minimum bias of  $0.10$  °C. It should be noted that the 105 year mean of observed temperature is about  $-4.50$  °C. It is also found that models with higher resolution do not always perform better than those with lower resolutions (such as the FGOALS-g2 model). For the seasonal SAT simulation, model biases in March–April–May (MAM) and June–July–August (JJA) are relatively small, while the bias in December–January–February (DJF) is high. Compared with the BCC-CSM 1.1 model, the GISS-E2-R model has the smaller bias in the seasonal SAT simulation.

The SAT observation has increased at a rate of about  $1.1$  °C/100 yrs during 1901–2005 (figure 2). Among the 24 GCMs, 12 models overestimate the warming trend, and the others overestimate. However, the warming trend differences



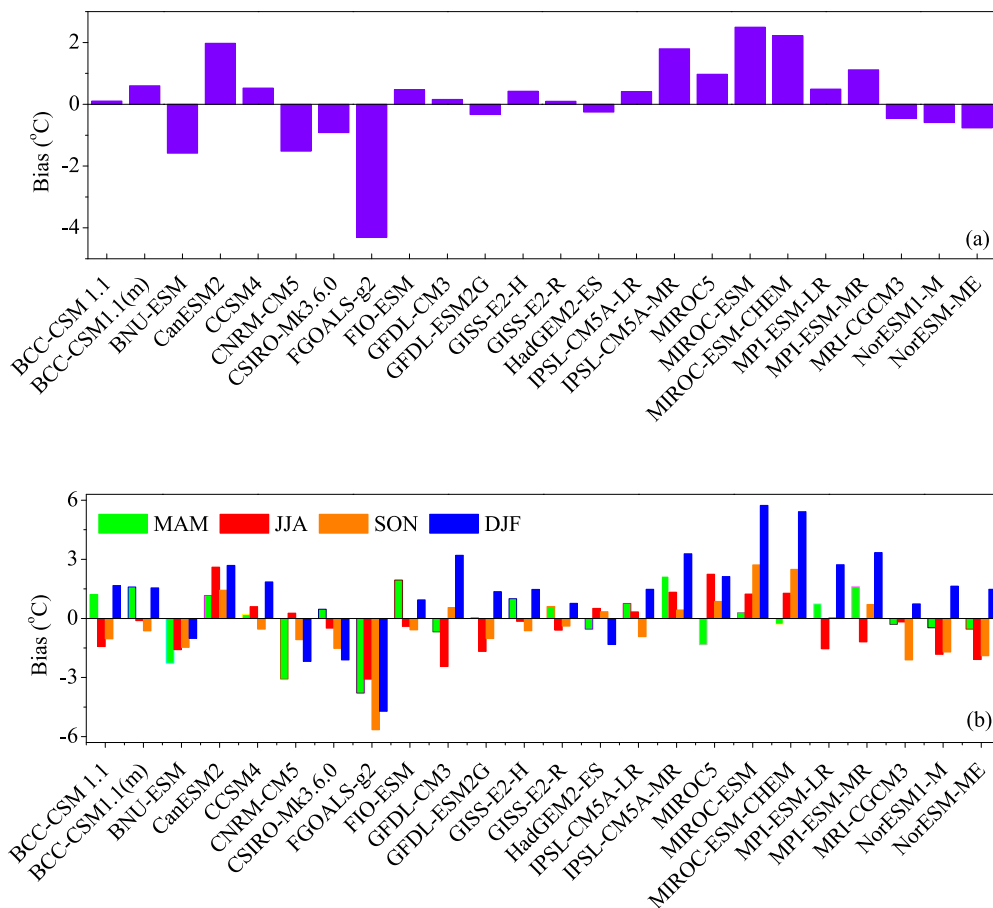


**Figure 1.** (a) Annual and (b) seasonal bias of different AR5 GCMs with regard to observed mean temperature in Northern Eurasia during 1901–2005.

between the observation and the overestimating models are generally larger than that from the underestimating model. The simulated warming trends by the IPSL-CM5A-LR and MRI-CGCM3 models are closest to the observations, and the maximum warming trend (approximately 2.76 °C/100 yrs) is simulated by the BNU-ESM model. It is widely recognized that if the worst impacts of climate change are to be avoided then the average rise in the surface temperature of the Earth needs to be less than 2 °C. Hence, we project the time when the global land mean SAT (without Antarctica) reaches a 2 °C increase relative to 2000 under different RCPs, and compare with the corresponding SAT increase over Northern Eurasia at that time (table 2). Under the RCP 2.6 scenario, six GCMs (CanESM2, GFDL-CM3, HadGEM2-ES, MIROC5, MIROC-ESM and MIROC-ESM-CHEM) show the global SAT will rise by 2 °C in this century. And only one GCM model (GISS-E2-R) estimates the global SAT will not increase by 2 °C within this century under RCP 4.5. The projected time by the remaining GCMs is dispersed from 2034 to 2081. All GCMs affirm that the global SAT will rise by 2 °C in this century under the RCP 8.5, and most of the models forecast that the projected time will occur from the 2030s–2050s. Under different scenarios, most of GCMs (except BCC-CSM1.1 (m), CSIRO-Mk3.6.0, GISS-E2-R and MPI-ESM-LR) believe the warming rate over the Northern Eurasia is

higher than the global warming average in this century. And some models (such as GFDL-CM3 in RCP 4.5 and MRI-CGCM3 in RCP 8.5) even show the warming in Northern Eurasia is more than twice faster than the global average.

### 2.2. Evaluation of temporal SAT simulation

Figure 3 shows the performance of the annual SAT simulation over the Northern Eurasia. The annual mean SAT observation increases during 1901–2005, and the warming has accelerated since the mid-20th century. Compared with the CMIP3 model, the CMIP5 model improves slightly in the annual SAT simulation, showing as closer to the observation point in the Taylor diagram (figure 3(a)). It is also indicated that most of the GCMs can approximate the trend of SAT, but the accuracy of annual SAT simulation is relatively low. The correlation coefficient *R* between each GCM simulation and the annual observation ranges from 0.20 to 0.56 (figure 3(a)). The ensemble results show that the ensemble technique can improve the temporal SAT simulation when compared to a single GCM (figure 3(b)). For multi-model ensemble simulation, the performances of the SMA, REA and BMA are similar since their outputs nearly overlap in the Taylor diagram. Comparing the weights generated by BMA and REA techniques, it is found that the model weights are similar but not identical. This is an interesting phenomenon that SMA,

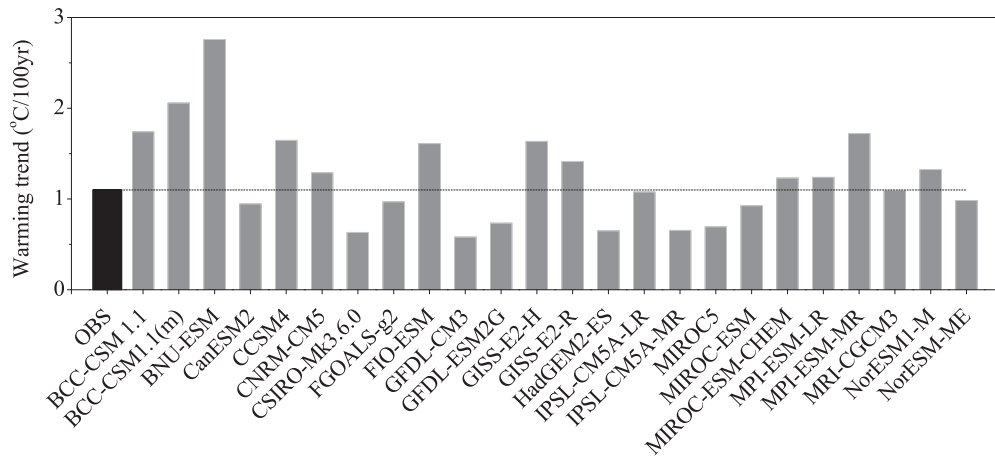


Figure 2. Warming trend for the observations (black bar, left) and each CMIP5 model during 1901–2005.

Table 2. The projected time when global land mean SAT increases 2 °C relative to 2000 under different RCPs and the corresponding SAT increases over Northern Eurasia.

Model	The year global mean SAT increases 2 °C relative to 2000			Increase in mean SAT over Northern Eurasia when global mean SAT increases 2 °C		
	RCP26	RCP45	RCP85	RCP26	RCP45	RCP85
BCC-CSM 1.1	×	2081	2052	×	2.90	2.41
BCC-CSM1.1(m)	×	2067	2049	×	1.66	1.87
BNU-ESM	×	2049	2039	×	3.99	2.72
CanESM2	2036	2036	2030	2.69	2.8	2.77
CCSM4	×	2063	2043	×	3.29	3.12
CNRM-CM5	×	2071	2053	×	3.29	2.68
CSIRO-Mk3.6.0	×	2054	2045	×	1.92	1.74
FGOALS-g2	×	2056	2039	×	3.01	2.93
FIO-ESM	×	2058	2059	×	2.27	1.81
GFDL-CM3	2027	2026	2025	3.61	4.5	3.09
GFDL-ESM2G	×	2052	2049	×	3.38	3.06
GISS-E2-H	×	2059	2043	×	3.08	3.32
GISS-E2-R	×	×	2054	×	×	1.89
HadGEM2-ES	2024	2034	2032	3.62	3.35	2.93
IPSL-CM5A-LR	×	2047	2042	×	3.55	3.11
IPSL-CM5A-MR	×	2060	2046	×	2.51	2.79
MIROC5	2041	2043	2034	2.11	2.32	2.17
MIROC-ESM	2045	2040	2033	3.14	2.60	2.56
MIROC-ESM-CHEM	2027	2027	2028	3.52	3.64	3.70
MPI-ESM-LR	×	2063	2042	×	1.23	1.06
MPI-ESM-MR	×	2061	2043	×	3.30	2.11
MRI-CGCM3	×	2077	2045	×	3.62	4.09
NorESM1-M	×	2045	2043	×	2.27	2.27
NorESM-ME	×	2052	2047	×	3.21	2.22

Symbol ‘x’ means the rise in global SAT will not reach 2 °C in this century.

REA and BMA generate very similar results, even though the ensemble members receive different weights through the three ensemble techniques.

Because a GCM cannot accurately reflect the actual annual SAT change (figure 3(b)), here we focus on the decadal SAT simulation (figure 4). It shows that GCM can catch the trend of 10-year moving average SAT over Northern

Eurasia. Compared with the annual scale, the correlation coefficients between the decadal SAT simulations and observation are increased, being primarily between 0.6 and 0.9; and the ensemble technique can improve the decadal SAT simulation further (figure 4(a)). Similar to figure 3(b), the decadal SAT changes simulated by three kinds of ensemble mean methods are almost the same (figure 4(b)). Besides

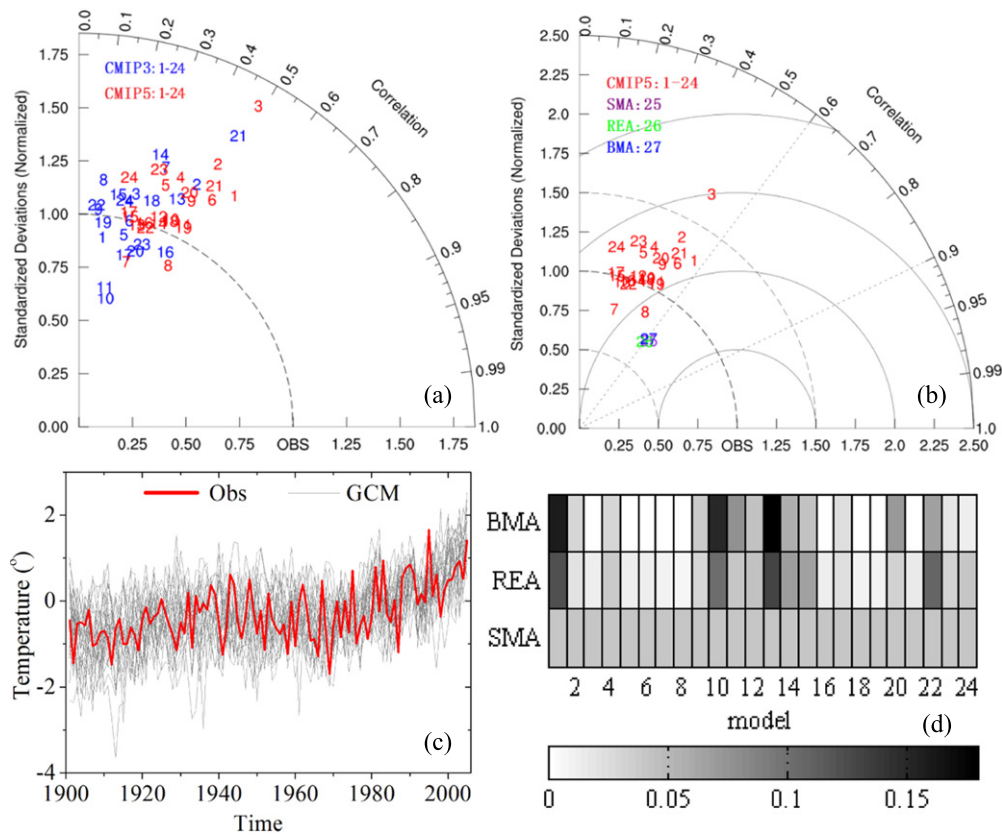


**Figure 3.** The performance of the annual SAT simulation over Northern Eurasia. (a) Taylor diagram for each model SAT simulation from CMIP5 (red) and CMIP3 (blue, model information see the online supplementary material ([stacks.iop.org/ERL/0/000000/mmedia](http://stacks.iop.org/ERL/0/000000/mmedia))) datasets; (b) comparison between annual SAT simulation from CMIP5 and their ensembles; (c) annual mean SAT anomalies from CMIP5 (relative to the 1970–1999); (d) weights of different ensemble processes.

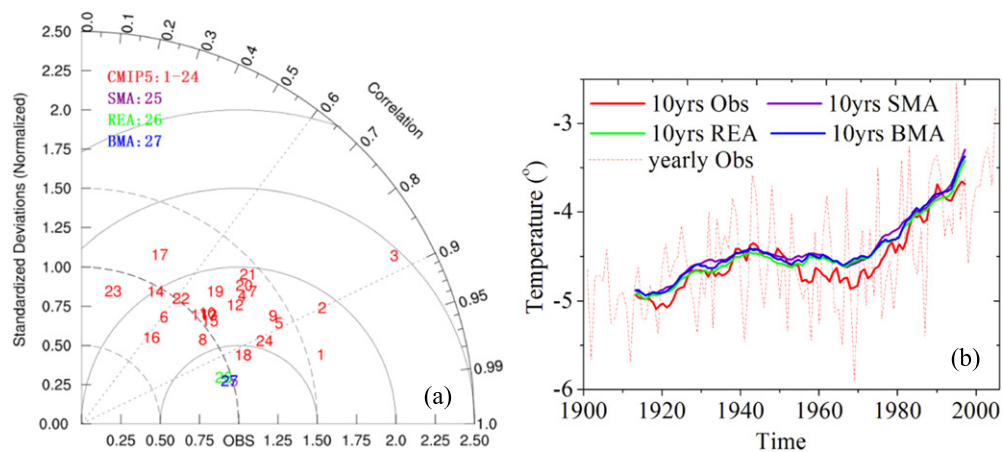


**Figure 4.** The performance of decadal SAT simulation. (a) Taylor diagram for each model and ensemble SAT simulation on decadal scale. (b) Ensemble for decadal SAT simulation.

ensemble average, uncertainty is another important skill score. Hence, the uncertainty of the multi-model ensembles during the period of 1901–2005 is also compared. Figure 5 shows the ensemble uncertainty of the simulated results with a 10 year moving average. It is indicated that the uncertainty generated by the BMA is the smallest among the three multi-model ensemble results for simulating the annual and seasonal SAT. In addition, the results show that the uncertainty in DJF is the largest over Northern Eurasia.

### 2.3. Projected SAT change in the 21st century

Considering the smallest uncertainty, the BMA method is applied to project the SAT change in the 21st century under the three future emission scenarios (RCP 2.6, RCP 4.5, RCP 8.5) (figure 6). Only the decadal SAT is projected, due to the poor performance on the annual scale. The BMA simulations show that the SAT of Northern Eurasia will increase remarkably over the 21st century. On average, the SAT over



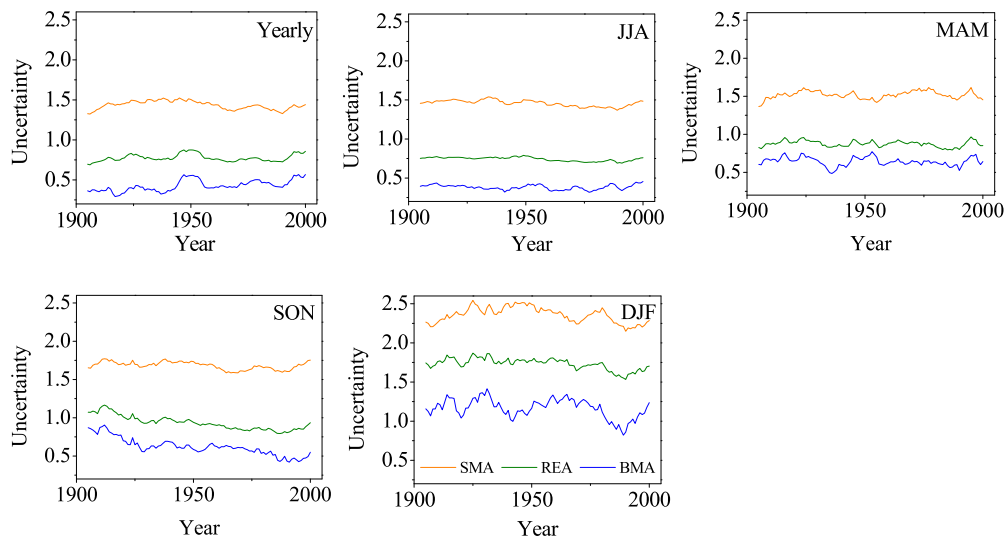


Figure 5. The ensemble uncertainty of annual and seasonal SAT simulated results with a 10-year moving average.

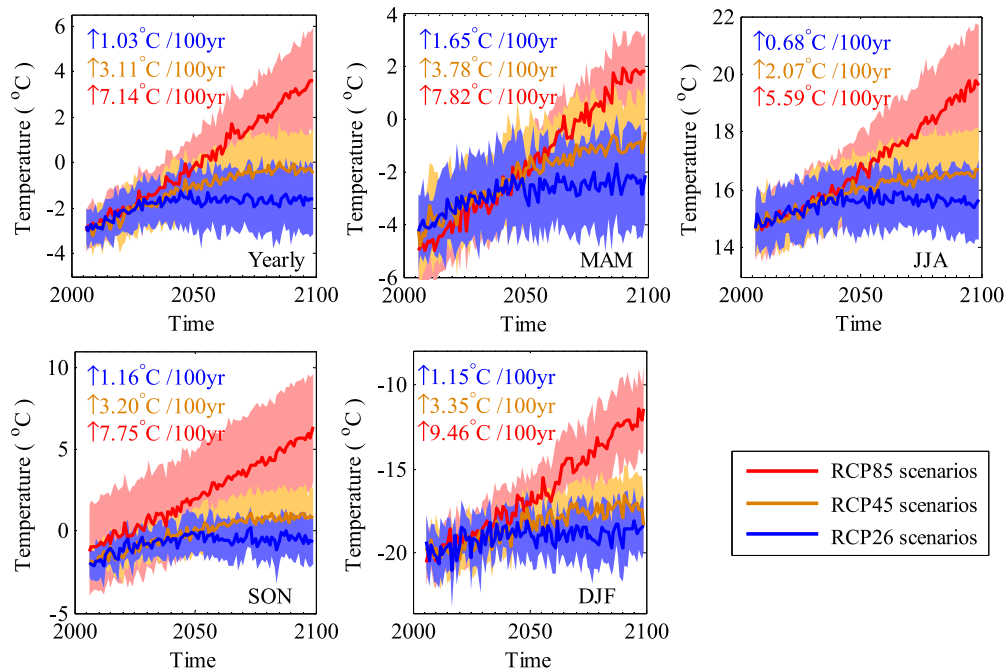
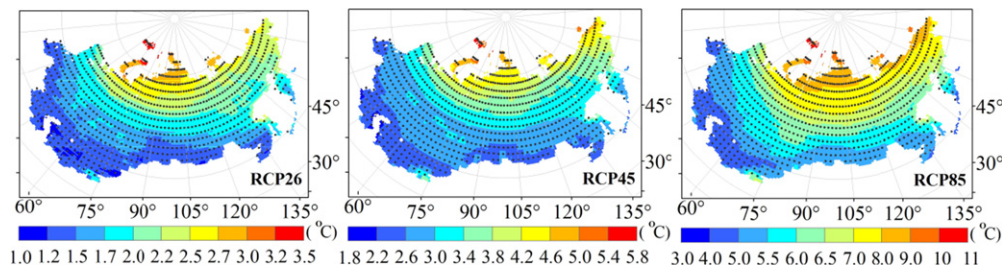


Figure 6. SAT projections over the 21st century using the BMA method. Shown are the evolutions under three emission scenarios derived by applying a 10 yr moving average. Solid lines are the Bayesian multi-model averages of SAT in Northern Eurasia under the scenarios RCP85 (red line), RCP45 (yellow line) and RCP26 (blue line). The color text indicates the average rate of warming under the scenarios RCP85 (red), RCP45 (yellow) and RCP26 (blue). Shading denotes the  $\pm 1$  standard deviation range of the BMA results with a 10-year moving average.

Northern Eurasia will rise by 1.03 °C/100 yr, 3.11 °C/100 yr and 7.14 °C/100 yr for the RCP 2.6, RCP 4.5 and RCP 8.5 scenarios, respectively. Under the RCP 2.6 and RCP 4.5 scenarios, the greatest contribution to the decadal warming is from MAM, while DJF is the largest contributor under the RCP 8.5 scenario. The warming trend slows down or even declines after 2050 under RCP 2.6. For the uncertainty of the SAT projections, it is found that the uncertainty of SAT projections increases with time in the 21st century, and the uncertainty under RCP 8.5 is larger than that under RCP 2.6 and RCP 4.5.

Figure 7 shows the projected annual mean SAT change for 2080–2099. The annual mean SAT in the last two decades of 21st century relative to 1986–2005 over Northern Eurasia will increase 1.92 °C, 3.25 °C and 6.40 °C under the RCP 2.6, RCP 4.5 and RCP 8.5 scenarios, respectively. It is found that the warming climate accelerates with increasing latitude. Grids with maximum SAT changes are concentrated in the Svalbard region of Norway under three scenarios, the corresponding changes are 3.61 °C, 5.57 °C and 10.24 °C under the RCP 2.6, RCP 4.5 and RCP 8.5, respectively.



**Figure 7.** Bayesian model averaging of annual mean SAT change (compared to 1986–2005 base period) for 2080–2099 under different scenarios. Stippling indicates regions where the BMA signal is greater than two standard of internal variability and where 90% of the models agree on the sign of change.

### 3. Discussion and conclusions

This study evaluates and compares the SAT change over Northern Eurasia using the outputs from the GCMs, SMA, REA and BMA, and projects the future SAT trend for different emission scenarios. The major findings of this study are summarized and discussed as follows:

(1) Most of the GCMs overestimate the annual mean temperature over Northern Eurasia. Similar results are also found in the Arctic (Chylek *et al* 2011), in the Northern hemisphere (Zhao *et al* 2013) and globally (Kim *et al* 2012). The forced and internal variation might contribute the overestimated warming in SAT simulation. It is reported that some CMIP5 models overestimate the responses to the increasing greenhouse gas and other anthropogenic forcing (IPCC 2013). The stratospheric aerosol concentration has increased over the past decade due to the volcanic eruptions, and has cooled global lower-atmosphere temperatures to a statistically significant degree (Santer *et al* 2014). However, none of the CMIP5 simulations takes this into account (Solomon *et al* 2011, Santer *et al* 2014). Moreover, some researchers think the inaccurate way that CMIP5 model handles clouds and water vapor is the main reason for the overestimation. It is found that the CMIP5 model tends to underestimate the cloud cover (Nam *et al* 2012) and stratospheric water vapor (Fyfe *et al* 2013a), both of which allow more sun to get in and then to heat up the planet during the simulation. Satellite observations suggest that climate models have ignored the negative feedbacks produced by clouds and water vapor (Christy *et al* 2010). The missing of these negative feedbacks diminishes the warming effects of carbon dioxide (Fyfe *et al* 2013a,b). Similarly to the CMIP3 (Miao *et al* 2013), the models with higher resolution do not always perform better than those with lower resolutions. Generally, the error of annual SAT simulation primarily comes from DJF, while the model biases in MAM and JJA are relatively smaller (figure 1(b), figure 3(b), figure 5). Most of the GCMs can approximate the decadal SAT trend, but the accuracy of annual SAT simulation is relatively low. The correlation coefficients *R* between each GCM simulation and the annual observations range from 0.20 to 0.56. Hence, direct use of the short-term output from

single GCM is not recommended. To model the short-term dynamic series, the effective techniques to improve the regional simulation accuracy should be considered in advance.

(2) The performances of the multi-model ensembles are superior to that of any single GCM. The Taylor diagram shows that all the multi-models ensemble techniques can improve the skill scores of simulations. The SAT changes in Northern Eurasia generated by SMA, REA and BMA are almost identical during 1901–2005. In general, the approach where model weights are determined by the model skill performs better than the method of equally weighing all models (e.g., Yun *et al* 2003, Tebaldi and Knutti 2007, Räisänen and Ylhäisi 2012). But some researches also obtained similar ensemble results calculated by different methods. Duan and Phillips (2010) analyze the global annual mean continental temperature and precipitation during 1980–1999, and find the results of the SMA and BMA are almost the same. This finding partially reflects the so-called ‘equifinality’ in which different combinations of model weights produce the same fit to the observation. In fact, the advantages of the uneven weighting ensemble method are mainly exhibited in narrowing the uncertainty (Giorgi and Mearns 2002, Duan and Phillips 2010, Hawkins and Sutton 2011). Comparing the annual and seasonal SAT uncertainties in the outputs of REA and SMA, the uncertainty generated by BMA is the smallest. Unequal weighting ensemble techniques contain the information from all participating models and embrace distinctly different physical parameterizations (Pincus *et al* 2008). Different model weight is also assigned according to its performance. Consequently, the unequal weight ensemble techniques moderate the uncertainties arising from different parameterizations and dynamical cores in the different GCMs (Zanis *et al* 2009).

(3) The SAT projections over Northern Eurasia show that SAT will increase in the 21st century by 1.03 °C/100 yr, 3.11 °C/100 yr and 7.14 °C/100 yr under the RCP 2.6, RCP 4.5 and RCP 8.5 scenarios, respectively. The warming accelerates with increasing latitude. All the maximum warming under the three scenarios is concentrated in the Svalbard region. Under the RCP 2.6 and RCP 4.5 scenarios, the greatest contribution to the decadal warming comes from MAM, and under the RCP

8.5 scenario, DJF becomes the greatest contributor. Compared with RCP 4.5 and RCP 8.5, the warming trend slows down or even starts declining after the 2050s under RCP 2.6. It is primarily because the RCP 2.6 scenario is designed to limit the increase of global mean temperature to 2 °C (van Vuuren *et al* 2011), and it has a peak in the radiative forcing at approximately 3 W m<sup>-2</sup> (approximately 400 ppm CO<sub>2</sub>) before 2100 and then declines to 2.6 W m<sup>-2</sup> by the end of the 21st century (approximately 330 ppm CO<sub>2</sub>) (Sillmann *et al* 2013). In addition, it is found that the uncertainty of the SAT projection outputs simulated by the BMA in the 21st century increases with time. The uncertainty change can be explained by its composition. The uncertainty in the SAT projection arises from three distinct sources: the internal variability of the climate system, the model uncertainty and the scenario uncertainty (Hawkins and Sutton 2009). In CMIP5, internal variability is roughly constant through time, and the other uncertainties grow with time, but at different rates (IPCC 2013). For scenario uncertainty, the spread between RCP scenarios is the dominant source of uncertainty by the end of the century (Hawkins and Sutton 2011). Overall, the uncertainty concluded using CMIP5 is not much changed from using CMIP3 (Knutti and Sedlacek 2013). Considering the mitigation and controllability of greenhouse gas, if we assume that the atmospheric concentrations of greenhouse gases decline quite rapidly under all RCPs in the next few decades, the scenario uncertainty may be smaller than that in the current projection. Not surprisingly, we are supposed to pay more attention to the internal variability and inter-model uncertainty in the near future.

GCM serves as a primary tool for studying and understanding climate change. In response to the SAT projections under different scenarios; it is important to make different adaptation and mitigation strategies in Northern Eurasia.

## Acknowledgements

The authors appreciate the valuable comments of Professor Pavel Ya Groisman and Dr Linyin Chen. Funding for this research was provided by the National Natural Science Foundation of China (no. 41001153), the National Key Basic Special Foundation Project of China (no. 2010CB951604), Beijing Higher Education Young Elite Teacher Project, and the State Key Laboratory of Earth Surface Processes and Resource Ecology. We are grateful to the Program for Climate Model Diagnosis and Intercomparison (PCMDI) for collecting and archiving the model data and to the Climate Research Unit (CRU) for collecting and archiving the observed climate data.

## References

- Allen C D *et al* 2010 A global overview of drought and heat-induced tree mortality reveals emerging climate change risks for forests *Forest Ecol. Manag.* **259** 660–84
- Bulygina O N, Groisman P Y, Razuvaev V N and Korshunova N N 2011 Changes in snow cover characteristics over Northern Eurasia since 1966 *Environ. Res. Lett.* **6** 045204
- Buser C M, Kunsch H R, Luthi D, Wild M and Schar C 2009 Bayesian multi-model projection of climate: bias assumptions and interannual variability *Clim. Dynam.* **33** 849–68
- Casanova S and Ahrens B 2009 On the weighting of multimodel ensembles in seasonal and short-range weather forecasting *Mon. Weather Rev.* **137** 3811–22
- Christy J R, Herman B, Pielke R, Klotzbach P, McNider R T, Hnilo J J, Spencer R W, Chase T and Douglass D 2010 What do observational datasets say about modeled tropospheric temperature trends since 1979? *Remote Sens.* **2** 2148–69
- Chylek P, Li J, Dubey M K, Wang M and Lesins G 2011 Observed and model simulated 20th century arctic temperature variability: canadian earth system model CanESM2 *Atmos Chem. Phys. Diss.* **11** 22893–907
- Coquard J, Duffy P B, Taylor K E and Iorio J P 2004 Present and future surface climate in the western USA as simulated by 15 global climate models *Clim. Dynam.* **23** 455–72
- Covey C, AchutaRao K M, Cubasch U, Jones P, Lambert S J, Mann M E, Phillips T J and Taylor K E 2003 An overview of results from the coupled model intercomparison project *Global Planet Change* **37** 103–33
- Dempster A P, Laird N M and Rubin D B 1977 Maximum likelihood from incomplete data via the EM algorithm *J. R. Stat Soc. B* **39** 1–38
- Duan Q Y and Phillips T J 2010 Bayesian estimation of local signal and noise in multimodel simulations of climate change *J. Geophys. Res.* **115** D18123
- Engler R and Guisan A 2009 MIGCLIM: predicting plant distribution and dispersal in a changing climate *Divers Distrib.* **15** 590–601
- Errasti I, Ezcurra A, Sáenz J and Ibarra-Berastegi G 2011 Validation of IPCC AR4 models over the Iberian peninsula *Theor. Appl. Climatol.* **103** 61–79
- Fyfe J C, von Salzen K, Cole J N S, Gillett N P and Vernier J P 2013a Surface response to stratospheric aerosol changes in a coupled atmosphere-ocean model *Geophys Res. Lett.* **40** 584–8
- Fyfe J C, Gillett N P and Zwiers F W 2013b Overestimated global warming over the past 20 years *Nat. Clim. Change* **3** 767–9
- Giorgi F and Mearns L O 2002 Calculation of average, uncertainty range, and reliability of regional climate changes from AOGCM simulations via the ‘reliability ensemble averaging’ (REA) method *J. Climate* **15** 1141–58
- Gosling S N, Lowe J A, McGregor G R, Pelling M and Malamud B D 2009 Associations between elevated atmospheric temperature and human mortality: a critical review of the literature *Clim. Change* **92** 299–341
- Gosling S N, Warren R, Arnell N W, Good P, Caesar J, Bernie D, Lowe J A, van der Linden P, O’Hanley J R and Smith S M 2011 A review of recent developments in climate change science. Part II: the global-scale impacts of climate change *Prog. Phys. Geog.* **35** 443–64
- Groisman P *et al* 2009 The Northern Eurasia Earth Science Partnership: an example of science applied to societal needs *B. Am. Meteorol. Soc.* **90** 671–88
- Groisman P and Soja A J 2009 Ongoing climatic change in Northern Eurasia: justification for expedient research *Environ. Res. Lett.* **4** 045002



- Groisman P Y, Knight R W, Razuvaev V N, Bulygina O N and Karl T R 2006 State of the ground: climatology and changes during the past 69 years over Northern Eurasia for a rarely used measure of snow cover and frozen land *J. Climate* **19** 4933–55
- Groisman P Y et al 2007 Potential forest fire danger over Northern Eurasia: changes during the 20th century *Global Planet Change* **56** 371–86
- Harris I, Jones P D, Osborn T J and Lister D H 2013 Updated high-resolution grids of monthly climatic observations *Int. J. Climatol.* **34** 623–42
- Hawkins E and Sutton R 2009 The potential to narrow uncertainty in regional climate predictions *B. Am. Meteorol. Soc.* **90** 1095–107
- Hawkins E and Sutton R 2011 The potential to narrow uncertainty in projections of regional precipitation change *Clim. Dynam.* **37** 407–18
- IPCC 2001 *Climate Change 2001: Third Assessment Report of the Intergovernmental Panel on Climate Change* (Cambridge: Cambridge University Press)
- IPCC 2007 Climate change 2007: the physical sciences basis *Contribution of Working Group I to the Fourth Assessment Report of the Intergovernmental Panel on Climate Change* ed S Solomon, D Qin, M Manning, Z Chen, M Marquis, K B Averyt, M Tignor and H L Miller (Cambridge: Cambridge University Press) p 966
- IPCC 2013 Climate change 2013: the physical science basis *Contribution of Working Group I to the Fifth Assessment Report of the Intergovernmental Panel on Climate Change* ed T F Stocker, D Qin, G K Plattner, M Tignor, S K Allen, J Boschung, A Nauels, Y Xia, V Bex and P M Midgley (Cambridge: Cambridge University Press)
- Kim H M, Webster P J and Curry J A 2012 Evaluation of short-term climate change prediction in multi-model CMIP5 decadal hindcasts *Geophys. Res. Lett.* **39** L10701
- Knutti R and Sedlacek J 2013 Robustness and uncertainties in the new CMIP5 climate model projections *Nat. Clim. Change* **3** 369–73
- Liu J P, Song M R, Horton R M and Hu Y Y 2013 Reducing spread in climate model projections of a september ice-free arctic *P. Natl. Acad. Sci. USA* **110** 12571–6
- Lobell D B, Burke M B, Tebaldi C, Mastrandrea M D, Falcon W P and Naylor R L 2008 Prioritizing climate change adaptation needs for food security in 2030 *Science* **319** 607–10
- McBean G, Alexeev G, Chen D, Førlund E, Fyfe J, Gorisman P Y, King R, Melling H, Vose R and Whitfield P H 2005 *Arctic Climate: Past and Present Arctic Climate Impact Assessment* (Cambridge: Cambridge University Press) pp 21–60
- Meinshausen M et al 2011 The RCP greenhouse gas concentrations and their extensions from 1765 to 2300 *Clim. Change* **109** 213–41
- Miao C Y, Duan Q Y, Sun Q H and Li J D 2013 Evaluation and application of bayesian multi-model estimation in temperature simulations *Prog. Phys. Geog.* **37** 727–44
- Miao C Y, Ni J R and Borthwick A G L 2010 Recent changes in water discharge and sediment load of the Yellow River basin, China *Prog. Phys. Geog.* **34** 541–61
- Miao C Y and Ni J R 2009 Variation of natural streamflow since 1470 in the Middle Yellow River, China *Int J Environ. Res. Public Health* **6** 2849–64
- Mitchell T D and Jones P D 2005 An improved method of constructing a database of monthly climate observations and associated high-resolution grids *Int. J. Climatol.* **25** 693–712
- Moss R H et al 2010 The next generation of scenarios for climate change research and assessment *Nature* **463** 747–56
- Mote P W and Salathe E P 2010 Future climate in the pacific northwest *Clim. Change* **102** 29–50
- Nam C, Bony S, Dufresne J L and Chepfer H 2012 The ‘too few, too bright’ tropical low-cloud problem in CMIP5 models *Geophys. Res. Lett.* **39** L21801
- Nowak D J 2010 Urban biodiversity and climate change *Urban Biodiversity and Design* ed N Müller, P Werner and J G Kelcey (Oxford: Wiley-Blackwell) pp 101–17
- Piao S L et al 2010 The impacts of climate change on water resources and agriculture in China *Nature* **467** 43–51
- Piao S L, Friedlingstein P, Ciais P, de Noblet-Ducoudre N, Labat D and Zaehle S 2007 Changes in climate and land use have a larger direct impact than rising CO<sub>2</sub> on global river runoff trends *P. Natl. Acad. Sci. USA* **104** 15242–7
- Pincus R, Batstone C P, Hofmann R J P, Taylor K E and Glecker P J 2008 Evaluating the present-day simulation of clouds, precipitation, and radiation in climate models *J. Geophys. Res.* **113** D14209
- Polyakov I V, Walsh J E and Kwok R 2012 Recent changes of arctic multiyear sea ice coverage and the likely causes *B. Am. Meteorol. Soc.* **93** 145–51
- Raftery A E, Gneiting T, Balabdaoui F and Polakowski M 2005 Using Bayesian model averaging to calibrate forecast ensembles *Mon. Weather Rev.* **133** 1155–74
- Räisänen J and Ylhäisi J 2012 Can model weighting improve probabilistic projections of climate change? *Clim. Dynam.* **39** 1981–98
- Robine J M, Cheung S L K, Le Roy S, Van Oyen H, Griffiths C, Michel J P and Herrmann F R 2008 Death toll exceeded 70 000 in Europe during the summer of 2003 *Cr. Biol.* **331** 171–5
- Rogelj J, Meinshausen M and Knutti R 2012 Global warming under old and new scenarios using IPCC climate sensitivity range estimates *Nat. Clim. Change* **2** 248–53
- Romanovsky V E, Sazonova T S, Balobaev V T, Shender N I and Sergueev D O 2007 Past and recent changes in air and permafrost temperatures in eastern Siberia *Global Planet Change* **56** 399–413
- Santer B D et al 2014 Volcanic contribution to decadal changes in tropospheric temperature *Nature Geosci.* **7** 185–9
- Sheffield J, Wood E F and Roderick M L 2012 Little change in global drought over the past 60 years *Nature* **491** 435–8
- Sillmann J, Kharin V V, Zwiers F W, Zhang X and Bronaugh D 2013 Climate extremes indices in the CMIP5 multimodel ensemble: part 2. future climate projections *J. Geophys. Res.* **118** 2473–93
- Solomon S, Daniel J S, Neely R R, Vernier J P, Dutton E G and Thomason L W 2011 The persistently variable ‘background’ stratospheric aerosol layer and global climate change *Science* **333** 866–70
- Sun Q H, Miao C Y, Duan Q Y, Kong D X, Ye A Z, Di Z H and Gong W 2014 Would the ‘real’ observed dataset stand up? a critical examination of eight observed gridded climate datasets for China *Environ. Res. Lett.* **9** 015001
- Tabari H and Taleae P H 2013 Moisture index for Iran: spatial and temporal analyses *Global Planet Change* **100** 11–9
- Taylor K E 2001 Summarizing multiple aspects of model performance in a single diagram *J. Geophys. Res.-Atmos.* **106** 7183–92
- Taylor K E, Stouffer R J and Meehl G A 2012 An overview of Cmp5 and the experiment design *B. Am. Meteorol. Soc.* **93** 485–98
- Tebaldi C and Knutti R 2007 The use of the multi-model ensemble in probabilistic climate projections *Philos. Trans. R. Soc. A* **365** 2053–75
- Tubiello F N, Soussana J F and Howden S M 2007 Crop and pasture response to climate change *P. Natl. Acad. Sci. USA* **104** 19686–90
- van Vuuren D P et al 2011 RCP2.6: exploring the possibility to keep global mean temperature increase below 2 °C *Clim. Change* **109** 95–116
- Wake D B and Vredenburg V T 2008 Are we in the midst of the sixth mass extinction? A view from the world of amphibians *P. Natl. Acad. Sci. USA* **105** 11466–73

- Weigel A P, Liniger M A and Appenzeller C 2008 Can multi-model combination really enhance the prediction skill of probabilistic ensemble forecasts? *Q. J. Roy. Meteor. Soc.* **134** 241–60
- Yang T, Hao X, Shao Q, Xu C Y, Zhao C, Chen X and Wang W 2011 Multi-model ensemble projections in temperature and precipitation extremes of the tibetan plateau in the 21st century *Global Planet Change* **80-81** 1–13
- Yang Y and Wendroth O 2014 State-space approach to analyze field-scale bromide leaching *Geoderma* **217-218** 161–72
- Yang Y, Wendroth O and Walton R J 2013 Field-scale bromide leaching as affected by land use and rain characteristics *Soil. Sci. Soc. Am. J.* **77** 1157–67
- Yun W T, Stefanova L and Krishnamurti T N 2003 Improvement of the multimodel superensemble technique for seasonal forecasts *J. Climate* **16** 3834–40
- Zanis P, Kapsomenakis I, Philandras C, Douvis K, Nikolakis D, Kanellopoulou E, Zerefos C and Repapis C 2009 Analysis of an ensemble of present day and future regional climate simulations for Greece *Int. J. Climatol* **29** 1614–33
- Zhao L, Xu J and Powell A M Jr 2013 Discrepancies of surface temperature trend in the CMIP5 simulations and observations on the global and regional scales *Clim. Past Diss.* **9** 6161–78
- Zhu X D, Zhuang Q L, Chen M, Sirin A, Melillo J, Kicklighter D, Sokolov A and Song L L 2011 Rising methane emissions in response to climate change in Northern Eurasia during the 21st century *Environ. Res. Lett.* **6** 045211